



Coláiste na Tríonóide, Baile Átha Cliath
Trinity College Dublin

Ollscoil Átha Cliath | The University of Dublin

Faculty of Engineering, Mathematics and Science
School of Physics

Nanoscience, Physics & Chemistry of Advanced Materials

Senior Sophister

Trinity Term 2018

PY4NP1

Comprehension and Problem Solving Paper

Paper Coordinator: Professor H. Zhang

Friday 4th May 2018

Physics - SNIAM

09.30 – 12.30

Instructions to Candidates:

Complete the comprehension exercise in **Section A** and **answer 6** questions from **Section B**

Section A accounts for 40% and **Section B** accounts for 60%

Tables of physical constants and relative atomic masses and a periodic table are attached.

Materials permitted for this examination:

Spectroscopic tables, character tables, Booklets of Formulae and Tables are available from the invigilator for all students who require them. Graph paper is also available.

Non-programmable calculators are permitted for this examination – please indicate the make and model of your calculator on each answer book used.

SECTION A

1. Read the short paper on pages 4 and 5 from [Nature Materials 17, 210-220 (2018)] and then answer the following questions/exercises (a)-(d)

(a) Write a brief summary of the article (not more than 1 page)

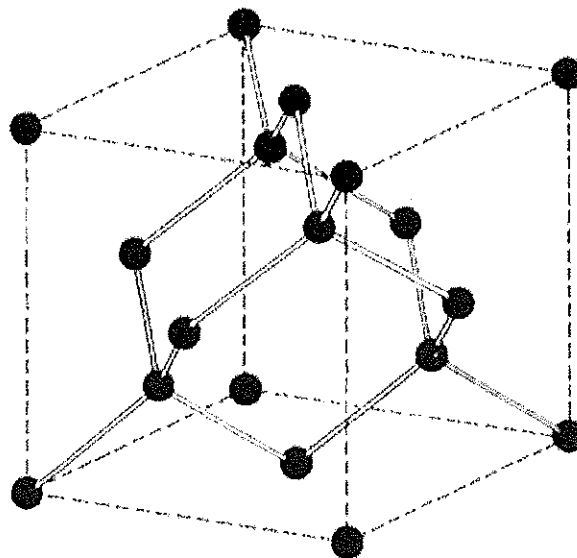
[10 marks]

(b) Briefly explain why the platelets are either parallel or perpendicular to each other in Fig. 1 of the short paper.

[2 marks]

(c) Figure 2 of the short paper are images viewed along the $[1\bar{1}0]$ direction. Consider the projection of the unit cell of the diamond structure along $[1\bar{1}0]$ direction (note: see the figure below, diamond is f.c.c. with $a = 3.57 \text{ \AA}$) and explain why a spatial resolution of better than 0.89 \AA has to be achieved in order to distinguish these defect structural models?

[3 marks]



(d) List the methodologies that enabled the identification of the structure model for the platelet defect and briefly explain what evidence each methodology provides for the structure identification.

[6 marks]

Note: Question 1 continued on next page

1. (e) List the challenges of imaging carbon materials by TEM and discuss the essential elements for the successful identification of the platelet defect structure by TEM?

[9 Marks]

- (f) What is the theory about the formation process of the platelet defect? How should one use microscopic studies to verify it? Assume the nitrogen atom to be located in the center of the tetrahedron of carbon atoms (i.e. substitutional). Consider the electronic state of the nitrogen atom and discuss the distortion of the tetrahedron.

[10 marks]

news & views

DIAMOND PLATELET STRUCTURE

Resolving the controversy

The structure of the platelet defect in diamond has been determined by transmission electron microscopy, distinguishing the best-matched atomic model that settles a long-standing debate.

Jannik Meyer

Diamonds are supposed to be highly transparent for visible light as well as parts of the infrared and ultraviolet spectrum, but in many cases they are not. It is defects in the diamond that make them absorb and emit photons in this spectral range, and also it's these same defects that make them interesting for a variety of scientific and technological applications. More than 100 different types of optically active defects are known in diamond, yet many of which have an unknown atomic configuration^{1,2}. One of these defects is the so-called platelet defect, a planar structure that lies on the {100} planes of the crystal and has a typical diameter of tens to hundreds of nanometres (Fig. 1). It is optically active in the infrared, with a frequency that depends on the size of the platelet³. The platelet defects exist in many natural and synthetic diamonds, while the exact atomic configuration of this defect has been subject to a significant controversy for more than half a century. Following X-ray diffraction studies in 1940 and subsequent transmission electron microscopy studies, several models have been proposed. Although to some extent the later models can be seen as a refinement of the earlier ones based on new experimental evidence, so far the experiments could not clearly distinguish between these theoretical structure models. Now, reporting in *Nature Materials*, Ezra Jaco Olivier and colleagues⁴ have settled very important aspects of this debate. Using atomically resolved scanning transmission electron microscopy (STEM), transmission electron microscopy (TEM), and electron energy-loss spectroscopy (EELS), they identified which, out of the set of candidate structures, agrees with reality. They concluded that the 'zigzag' model (Fig. 2) proposed in ref. ⁵ is the experimentally favoured configuration, and that the other candidates can be ruled out. In this model, interstitials of carbon or nitrogen are arranged at alternating (zigzag) sites, as indicated by the blue arrows in Fig. 2 for a platelet viewed along the [110] direction. The spectroscopic analysis also confirmed earlier studies that the platelet is

primarily composed of carbon, but does also contain a small fraction of nitrogen.

The work of Olivier and co-workers was made possible by recent advances in aberration-corrected electron microscopy, which enabled imaging of the platelets with sub-ångström spatial resolution and a sufficiently high contrast transfer. Imaging carbon materials by TEM or STEM is particularly challenging because the light atoms have a low contrast, are easily displaced by the energetic electron irradiation, and are particularly 'small' — that is, the interatomic distances that need to be resolved are shorter than those of most other elements. Electron microscopy is now sufficiently powerful to resolve the fine details in the extended defects in diamond, such as the platelet^{4,6}. Figure 2 highlights some aspects of the images that were obtained by Olivier and colleagues: not only does the spatial resolution allow resolving atomic columns with a projected distance of only 0.89 Å, but also the much weaker features within the defect can be separated and detected above the experimental noise level, in order to distinguish different models. In this context it is important to reiterate that along with higher spatial resolution, aberration correction in TEM or STEM also results in more contrast for weakly scattering features like the ones indicated by blue arrows in Fig. 2, which otherwise are hidden in the proximity of strongly scattering ones. Last but not least, aberration correction reduces 'nonlocal' effects in the images (contrast of the structure appearing away from its true location, due to contrast delocalization in TEM⁷ or probe tails in STEM⁸), which is often critical for an unambiguous interpretation. All of these were essential elements for the successful identification of the platelet defect structure.

Most of the knowledge about defects in diamond stems from the interplay of various spectroscopic methods and extensive modelling, and it will be interesting to see what role electron microscopy can play in the future. Nitrogen is the most common impurity in diamond, and probably the

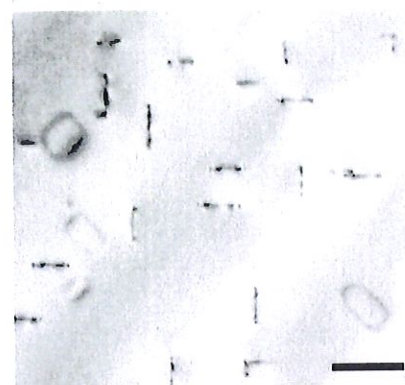


Fig. 1 | Transmission electron microscopy (TEM) image of platelet defects in a diamond. The platelets are seen edge-on and the image is rotated so that they appear either horizontally or vertically — never at an angle because the platelets are aligned with the crystal axes. Scale bar, 100 nm. Credit: adapted from ref. ⁴; Macmillan Publishers Ltd.

most well-known point defects in diamond are the nitrogen centre and nitrogen-vacancy centre — the latter has gained considerable attention recently due to its optical transition being extremely sensitive to external perturbations and its potential applications in quantum computing⁹. The platelets, in contrast, are an extended defect structure that are thought to arise from an agglomeration of nitrogen-containing defects into a planar geometry^{3,9}, although most of the nitrogen appears to escape in the process. The resulting chemical composition with a small amount of nitrogen among predominant carbon was also confirmed by the spectroscopic analysis of Olivier and colleagues⁴. Unfortunately, the formation process and the role of nitrogen in it still remain somewhat unclear, and further microscopic studies at different stages of the platelet formation might shed light on this point. Now that the platelet can be imaged so clearly, a most intriguing question is whether other defects in diamond, especially point defects, will become accessible by

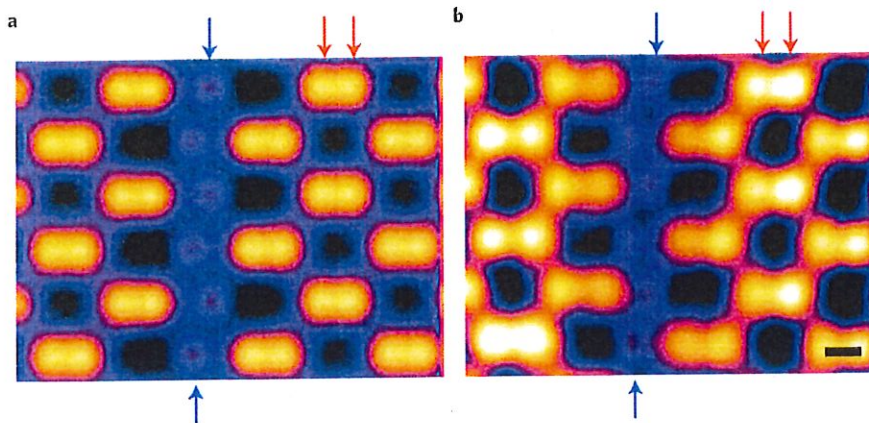


Fig. 2 | Comparison between theoretical simulation and experimental result of the platelet structure viewed along the $[1\bar{1}0]$ direction. **a**, Simulated image of the zigzag model structure. **b**, Experimental STEM image. The red arrows indicate two atomic columns with a separation of only 0.89 Å. The blue arrows indicate the location of the platelet, where in this particular view a set of weak features can be observed that allows one to distinguish the zigzag model from the other candidates. Scale bar, 1 Å. Credit: adapted from ref. 4, Macmillan Publishers Ltd.

electron microscopy. While nitrogen centres or nitrogen–vacancy centres have been imaged in graphene^{10,11}, such structures would be masked if they are embedded in a thick three-dimensional sample that possibly also has an amorphous cover layer. Hence,

going from the extended to the point defects still entails some formidable challenges lying ahead — for example, in sample preparation and radiation damage prevention. Uncovering the vast zoo of defects with unknown structures would

open new doors for tailoring optical and electronic properties of diamond. The work of Olivier and colleagues is a remarkable step forward for characterizing this challenging material, and it also highlights a promising avenue to study defects in diamond where the identification of the platelet structure can be seen as a starting point. □

Jannik Meyer

Physics of Nanostructured Materials Group,
University of Vienna, Vienna, Austria.
e-mail: jannik.meyer@univie.ac.at

Published online: 21 February 2018
<https://doi.org/10.1038/s41563-018-0026-4>

References

1. Zaitsev, A. M. *Optical Properties of Diamond: A Data Handbook* (Springer, Berlin, 2001).
2. Jelezko, F. & Wrachtrup, J. *Phys. Status Solidi A* **203**, 3207–3225 (2006).
3. Kiflawi, I., Bruley, J., Luyten, W. & Van Tendeloo, G. *Philos. Mag. Part B* **78**, 299–314 (1998).
4. Olivier, E. J. et al., *Nat. Mater.* <https://doi.org/10.1038/s41563-018-0024-6> (2018).
5. Barry, J., Bursill, L. & Hutchison, J. *Phil. Mag. A* **51**, 15–49 (1985).
6. Korneychuk, S., Turner, S., Abakumov, A. & Verbeeck, J. in *Proc. European Microscopy Congress* 331–332 (2016).
7. Lentzen, M. et al. *Ultramicroscopy* **92**, 233–242 (2002).
8. Kirkland, E. J. *Ultramicroscopy* **111**, 1523–1530 (2011).
9. Kiflawi, I. & Bruley, J. *Diam. Relat. Mater.* **9**, 87–93 (2000).
10. Meyer, J. C. et al. *Nat. Mater.* **10**, 209–215 (2011).
11. Lin, Y.-C. et al. *Nano Lett.* **15**, 7408–7413 (2015).

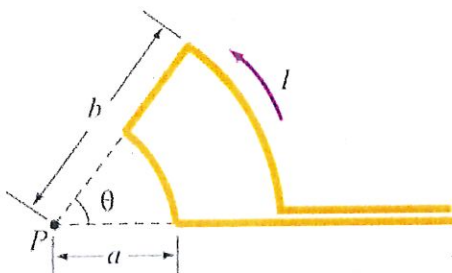
SECTION B

1. A heat engine working between heat reservoirs at 900 K and 580 K produces 460 J of work per cycle for a heat input of 1900 J.
- (a) Compare the efficiency of this engine to that of a Carnot engine. [5 marks]
- (b) Discuss the steps involved in functioning of the Carnot engine. [5 marks]
2. (a) Use Gauss's law to show that the electric field E at the surface of cylindrical column of charge of radius r is given by $E = \frac{\lambda}{2\pi\epsilon_0 r}$, where λ is the charge density per unit length.
- (b) A collimated electron beam of electrons is aimed at a phosphor screen 1 m away. The initial diameter of the electron beam is 2 mm, the electron velocity is $5 \times 10^4 \text{ m s}^{-1}$ and the beam current is $1 \mu\text{A}$. Estimate the diameter of the beam when it reaches the phosphor. [10 marks]
3. A $^1\text{H}^{19}\text{F}$ molecule has a bond length of 92 pm. Estimate the value of rotational state J required for this molecule to have the rotational kinetic energy equivalent to that of a hydrogen atom in the 2p state. You may assume that the probability density for the electron in the 2p state of hydrogen has a maximum at a distance of $4a_0$ from the hydrogen nucleus, where a_0 represents the Bohr radius. [10 marks]

4. A drone has mass m , rotor blades of area A and is hovering in air of density ρ .
- (a) With the assumption that the air driven downwards by the rotors is uniformly accelerated from rest to a velocity v across the area A , use the associated *rate of change of air momentum* to find an expression for v in terms of the weight of the drone. **Hint:** Consider how to define the volume or mass of air accelerated per unit time.
- (b) If all the rotor energy is used to give kinetic energy to the air, find an expression for the power required to enable the drone to hover.
- (c) Calculate the power required if $m = 1$ kg, $A = 5 \times 10^{-2}$ m² and $\rho = 1.2$ kg m⁻³
- (d) If the drone is powered by a 12 V, 3 Amp hr battery, for how long can it fly?
[10 marks]
5. (a) Derive an expression for the ratio of rate constants if the temperature is changed from a value T to $T + \Delta T$. Assume that the activation energy E_A remains constant over the temperature range T and $T + \Delta T$.
[5 marks]
- (b) If the numerical value of the activation energy is 50 kJ mol⁻¹ what is the ratio of the rate constants?
[5 marks]

6. (a) Use the Biot-Savart law, or otherwise, to calculate the magnetic field at the center of a current carrying loop of radius R .

- (a) Calculate the magnitude and direction of the magnetic field created by a current $I=1\text{ A}$ in the wire shown at a point P which is at the center of two arcs of wire at differing radii a and b and connected by radial wires to each other and to the source of current. The distances $a=2\text{ cm}$ and $b=4\text{ cm}$ and the angle $\theta=1\text{ rad}$.



Hint: The Biot-Savart law is $d\vec{B} = \frac{\mu_0 I}{4\pi} \frac{d\vec{s} \times \hat{r}}{r^2}$ where $d\vec{s}$ is in an element along the current carrying conductor, r the radial distance to this element, \hat{r} the unit position vector of this element; integrating gives $\vec{B} = \frac{\mu_0 I}{4\pi} \int \frac{d\vec{s} \times \hat{r}}{r^2}$.

[10 marks]

7. It has been suggested that H_3^+ , thought to exist in interstellar space, adopts a perfectly trigonal structure. Assuming this to be the case predict the Infra-Red and Raman active vibrational modes using group theoretical means.

[10 marks]

8. While in the past many people used to think that the Earth was flat, some still hold this belief.
- (a) List two persuasive physics arguments or observations that would counter this hypothesis; however limit your choice of arguments or observations to those that can be made from the surface of the Earth.
- (b) Imagine that the Earth is indeed not a sphere of radius R , but an infinite plate of thickness H . What value of H is needed to allow the same gravitational acceleration to be experienced on the surface of the actual Earth? Express this in terms of R . (Assume that the Earth's density is uniform and equal in the two models.)

Hint: The laws of gravitational and electrostatic fields are very similar. One could make use of this similarity and apply Gauss's law. You only need to know the radius of the Earth.

[10 marks]

9. (a) Consider a hypothetical diatomic hydrocarbon molecule comprised of one C-H bond and consider its deuterated analogue, C-D. Given that the C-H molecule has a vibrational stretching frequency of 3000 cm^{-1} and a bond dissociation energy of 420 kJ mol^{-1} , estimate the dissociation energy of the C-D molecule. Illustrate your answer carefully sketching the potential energy function for the diatomic system showing the magnitude of the dissociation energies for the two molecules.
- (b) Suppose these molecules undergo a reaction in which the C-H and C-D bonds are broken in the rate determining step. Estimate the maximum value of primary isotope effect at room temperature and describe the conditions under which this value can be realised.

Note (if not already provided) $\tilde{\nu} = \nu/c$

[10 marks]

10. In their classic experiment, Davisson and Germer directed an electron beam on to a nickel crystal at normal incidence and placed a detector at an angle θ from the beam. When the electrons were accelerated by a voltage of 54 volts, they observed strong reflection of these electrons into an angle $\theta = 50^\circ$. Calculate the atomic spacing on the surface and the lattice spacing in the nickel crystal if this was the nickel (111) surface of the fcc lattice.

[10 marks]

11. **M** and **M*** are group 1 and group 13 metals respectively. **M** can react directly with dinitrogen forming nitride. The reaction of **M** with hydrogen results in the corresponding metal hydride **A**. The reaction between metal **M*** and bromine yields product **B**, which has a dimeric structure. The treatment of **B** with 8 equivalents of hydride **A** results in a highly reactive product **C**, which reacts violently with water. Identify **M**, **M***, **A**, **B** and **C** giving your reasoning. Write balanced equations for all of the reactions above.

[10 marks]

12. (a) Light is directed at normal incidence onto a thin film of zinc selenide ($n=2.7$) on glass ($n=1.5$). Explain the conditions for a minimum, or a maximum, in *reflectance* from this thin film due to interference effects. Draw diagrams or give equations as necessary illustrating a maximum and minimum.
- (b) The *transmission* spectrum of a thin film of zinc selenide on glass obtained at normal incidence through the stack show successive *maxima* in transmission at 719.5 nm, 575.6 nm and 480 nm and *minima* in transmission at 822.3 nm, 639.6 nm and 523.3 nm. Calculate the thickness of the film.

[10 marks]

Hint: you may need to consider under what circumstances a phase change occurs when light is reflected off an interface based on change of refractive indices of the materials at that interface. You may assume there is no absorption or scattering and all the light is either reflected or transmitted.

Use the following values for fundamental constants, conversion factors, relative atomic masses and other data for examination purposes:

Constants

Gas Constant	$R = 8.314 \text{ J K}^{-1} \text{ mol}^{-1}$
Boltzmann's Constant	$k_B = 1.381 \times 10^{-23} \text{ J K}^{-1}$
Planck's Constant	$h = 6.626 \times 10^{-34} \text{ J s}$ $\hbar = h/2\pi = 1.055 \times 10^{-34} \text{ J s}$
Velocity of light	$c = 2.998 \times 10^8 \text{ m s}^{-1}$
Charge of electron	$e = -1.602 \times 10^{-19} \text{ C}$
Rest mass of electron	$m_e = 9.109 \times 10^{-31} \text{ kg}$
Rest mass of proton	$m_p = 1.673 \times 10^{-27} \text{ kg}$
Atomic Mass Unit	$1 \text{ u} = 1.66054 \times 10^{-27} \text{ kg}$
Vacuum permittivity	$\epsilon_0 = 8.854 \times 10^{-12} \text{ J}^{-1} \text{ C}^2 \text{ m}^{-1}$
Vacuum permeability	$\mu_0 = 4\pi \times 10^{-7} \text{ J s}^2 \text{ C}^{-2} \text{ m}^{-1}$
Bohr magneton	$\beta = 9.274 \times 10^{-24} \text{ J T}^{-1}$
Nuclear magneton	$\beta_n = 5.051 \times 10^{-27} \text{ J T}^{-1}$
Rydberg constant	$R_\infty = 2.178 \times 10^{-18} \text{ J} = 1.097 \times 10^5 \text{ cm}^{-1}$
Avogadro's constant	$N_A = 6.022 \times 10^{23} \text{ mol}^{-1}$
Faraday constant	$F = N_A e = 9.648 \times 10^4 \text{ C mol}^{-1}$
Bohr radius	$a_0 = 5.292 \times 10^{-11} \text{ m}$
Molar volume at S.T.P.	$M_v = 22.414 \text{ dm}^3 \text{ mol}^{-1}$

Conversion factors etc.

$1 \text{ eV} = 1.602 \times 10^{-19} \text{ J} = 9.648 \times 10^4 \text{ J mol}^{-1}$
$1 \text{ cm}^{-1} = 1.986 \times 10^{-23} \text{ J} = 11.96 \text{ J mol}^{-1} = 1.240 \times 10^{-4} \text{ eV}$
$1 \text{ \AA} = 0.1 \text{ nm} = 10^{-10} \text{ m}$
$1 \text{ standard atmosphere} = 1.013 \times 10^5 \text{ N m}^{-2} \text{ (Pa)} = 760 \text{ torr} = 1013 \text{ mbar}$
$1 \text{ L} = 1 \text{ dm}^3 = 10^{-3} \text{ m}^3$
$1 \text{ Debye (D)} = 3.336 \times 10^{-30} \text{ C m}$
$1 \text{ calorie} = 4.184 \text{ J}$
$R = 8.314 \text{ J K}^{-1} \text{ mol}^{-1} = 8.206 \times 10^{-2} \text{ L atm K}^{-1} \text{ mol}^{-1}$

Approximate values of relative atomic masses

(Values in brackets are mass numbers of longest lived isotopes).

Ac (227)	Ge 72.6	Po (209)
Ag 107.9	H 1.0	Pr 140.9
Al 27.0	He 4.0	Pt 195.1
Am (243)	Hf 178.5	Pu (244)
Ar 40.0	Hg 200.6	Ra (226)
As 74.9	Ho 164.9	Rb 85.5
At (210)	I 126.9	Re 186.2
Au 197.0	In 114.8	Rh 102.9
B 10.8	Ir 192.2	Rn (222)
Ba 137.3	K 39.1	Ru 101.1
Be 9.0	Kr 83.8	S 32.0
Bi 209.0	La 138.9	Sb 121.8
Bk (247)	Li 6.9	Sc 45.0
Br 79.9	Lu 175.0	Se 79.0
C 12.0	Lw (257)	Si 28.1
Ca 40.1	Md (258.1)	Sm 150.4
Cd 112.4	Mg 24.3	Sn 118.7
Ce 140.1	Mn 54.9	Sr 87.6
Cf (242.1)	Mo 95.9	Ta 180.9
Cl 35.5	N 14.0	Tb 158.9
Cm (247)	Na 23.0	Tc (97.9)
Co 58.9	Nb 92.9	Te 127.6
Cr 52.0	Nd 144.2	Tl 204.4
Cs 132.9	Ne 20.2	Th 232.0
Cu 63.5	Ni 58.7	Ti 47.9
Dy 162.5	No (259.1)	Tm 168.9
Er 167.3	Np (237)	U 238.0
Es (252.1)	O 16.0	V 50.9
Eu 152.0	Os 190.2	W 183.9
F 19.0	P 31.0	Xe 131.3
Fe 55.9	Pa (231)	Y 88.9
Fm (257)	Pb 207.2	Yb 173.0
Fr (223)	Pd 106.4	Zn 65.4
Ga 69.7	Pm (145)	Zr 91.2
Gd 157.3		

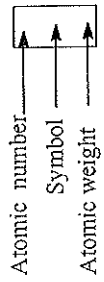
The Periodic Table of the Elements

18

1

1 1.0079 H	2 He 4.0026																				
3 6.941 Li	4 9.01218 Be	5 10.81 B	6 12.011 C	7 14.0067 N	8 15.9994 O	9 18.9984 F	10 20.179 Ne														
11 22.98977 Na	12 24.305 Mg	13 26.9815 Al	14 28.0855 Si	15 30.9738 P	16 32.06 S	17 35.453 Cl	18 39.948 Ar														
19 39.0983 K	20 40.08 Ca	21 44.9559 Sc	22 47.88 Ti	23 50.9415 V	24 51.996 Cr	25 54.938 Mn	26 55.847 Fe	27 58.9332 Co	28 58.99 Ni	29 63.546 Cu	30 65.38 Zn	31 69.72 Ga	32 72.59 Ge	33 74.9216 As	34 78.96 Se	35 79.904 Br	36 83.80 Kr				
37 85.4678 Rb	38 87.62 Sr	39 88.9059 Y	40 91.22 Zr	41 92.9064 Nb	42 95.94 Mo	43 97.9 Tc	44 101.07 Ru	45 102.9055 Rh	46 106.42 Pd	47 107.868 Ag	48 112.41 Cd	49 114.82 In	50 118.69 Sn	51 121.75 Sb	52 127.60 Te	53 126.9045 I	54 131.29 Xe				
55 132.9054 Cs	56 137.33 Ba	57 138.9055 #La	72 178.49 Hf	73 180.9479 Ta	74 183.85 W	75 186.207 Re	76 190.2 Os	77 192.22 Ir	78 195.08 Pt	79 196.9665 Au	80 200.59 Hg	81 204.383 Tl	82 207.2 Pb	83 208.9804 Bi	84 209 Po	85 210 At	86 222 Rn				
87 (223) Fr	88 226.025 Ra	89 227.0278 *Ac																			

Key



() mass numbers of most stable isotope

LANTHANUM SERIES

58	59	60	61	62	63	64	65	66	67	68	69	70	71
Ce	Pr	Nd	Pm	Sm	Eu	Gd	Tb	Dy	Ho	Er	Tm	Yb	Lu
140.12	140.9077	144.24	(145)	150.36	151.96	157.25	158.9254	162.50	164.9304	167.26	168.9342	173.04	174.967

* ACTINIUM SERIES

90	91	92	93	94	95	96	97	98	99	100	101	102	103
Th	Pa	U	Np	Pu	Am	Cm	Bk	Cf	Es	Fm	Md	No	Lr
232.0381	231.0359	238.0389	237.0482	(244)	(243)	(247)	(247)	(242.1)	(254)	(257)	(258.1)	(259.1)	(260)